Synthesis, Characterization, and Reactivity of Group 12 Metal Thiocarboxylates, $M(SOCR)_2Lut_2$ [M = Cd, Zn; R = CH_3, $C(CH_3)_3$; Lut = 3,5-Dimethylpyridine (Lutidine)]

May D. Nyman, Mark J. Hampden-Smith,* and Eileen N. Duesler

Center for Micro-Engineered Materials and Department of Chemistry, University of New Mexico, Albuquerque, New Mexico 87131

Received July 3, 1996[⊗]

A series of group 12 metal thiocarboxylate species, $M(SOCR)_2Lut_2$ [M = Cd, Zn; R = CH_3, $C(CH_3)_3$; Lut = 3,5-dimethylpyridine (lutidine)], were synthesized to investigate their potential to act as precursors for the formation of metal sulfide materials. These species were expected to undergo thiocarboxylic anhydride elimination to give stoichiometric metal sulfides and remove the organic supporting ligands cleanly. These species were characterized by ^1H, ^{13}C, and (where appropriate) ^{113}Cd NMR spectroscopies, TGA, elemental analysis, and single-crystal X-ray diffraction. The spectroscopic and analytical data were consistent with the formulas identified above, and in the solid state the compounds are monomeric with approximate tetrahedral metal coordination environments and monodentate S-bond thiocarboxylate ligands. Crystal data for $Cd(SOCCH_3)_2Lut_2$: crystallized in the triclinic space group $P\bar{1}$, with $a = 8.267(1)$ Å, $b = 9.467(1)$ Å, $c = 14.087(1)$ Å, $\alpha = 94.04(1)°$, $\beta = 91.49(1)°$, $\gamma = 104.03(1)°$, and $Z = 2$. Thermal decomposition of these compounds in the solid state or in solution resulted in formation of the corresponding metal sulfide at low temperatures, as seen by powder X-ray diffraction. Evidence for thiocarboxylic anhydride elimination was documented by NMR in solution phase reactions. The effects on thiocarboxylic anhydride elimination, resulting from varying M, R, or solvent media, were examined by heating NMR tube solutions of $M(SOCR)_2Lut_2$ in pyridine or toluene. Heating toluene or pyridine solutions of $Cd(SOCCH_3)_2Lut_2$ resulted in formation of nanocrystalline, sphalerite CdS, as determined by X-ray diffraction and TEM. These preliminary reactivity studies have revealed the great potential of this highly tailorable chemical system as precursors to group 12 metal sulfido species.

Introduction

Group 12 metal sulfide materials that include powders, films, nanoclusters, and molecular clusters have generated a great deal of scientific and technological interest for a number of different reasons. The semiconducting nature of these materials has led to fundamental interest in the synthesis of molecular clusters and nanoclusters to investigate size-dependent structure−property relationships. Their absorption properties in the UV and visible region of the electromagnetic spectrum have led to extensive uses as optical coatings[1,2] in solar cell technology, and they are excellent host lattices for luminescent materials used in display applications.[3,4]

The group 12 metal sulfides, in particular Zn and Cd, are of fundamental interest because they afford a rare opportunity to study the general aspects of structure−property relationships at length scales that vary from "molecules to materials" due to the structural similarities between molecular clusters,[5−7] nanoclusters,[8] and extended solids.[9] This is the result of the strong thermodynamic driving force to form MS units with tetrahedral coordination of both M and S, which is the basic structural building block of the bulk MS material. Molecular clusters,[5,10−12] nanoclusters,[7,13,14] and extended solids have generally been synthesized by independent chemical routes.

This paper describes the synthesis, characterization, and reactivity of a new class of precursors to metal sulfide materials, the group 12 metal thiocarboxylates, $M(SOCR)_2L_2$ (M = Zn, Cd, R = alkyl, aryl; L = Lewis base), which can undergo reactions such as thiocarboxylic anhydride elimination, shown in eq 1, to form "MS", which is the basic unit of an extended solid, molecular cluster, or nanocluster.

$$2M(SOCR)_2L_2 \rightarrow [(RCOS)M{-}S{-}M(SOCR)]L_2 + S(COR)_2 \quad (1)$$

$$[(SOCR)M{-}S{-}M(SOCR)]L_2 \rightarrow 2MS + (RCO)_2S + 2L \quad (2)$$

This strategy should be suitable for the synthesis of Zn, Cd, or mixed $Zn_{1-x}Cd_x$ materials. This reaction is likely to be subtly influenced by the steric and electronic effects of the solvent, R, M, and L. We have previously reported the synthesis and characterization of some metal thiocarboxylate compounds including $Cd(SOCCH_3)_2TMEDA$ and $Zn(SOCCH_3)_2TMEDA$ (TMEDA = *N,N,N,N*-tetramethylethylenediamine) and their use as precursors for aerosol-assisted (AA)CVD of CdS, ZnS, and $Cd_{1-x}Zn_xS$ thin films at extremely low temperatures (100−225

* Author to whom correspondence should be addressed.
⊗ Abstract published in *Advance ACS Abstracts,* April 15, 1997.

(1) Hovel, H. J. *Semiconductors and Semimetals, Vol 11: Solar Cells*; Academic: New York, 1975.
(2) Kukimoto, H. *J. Cryst. Growth* **1990**, *101*, 953.
(3) *Electronic Materials*; Braithwaite, N., Weaver, G., Eds.; The Open University: London, 1990.
(4) Bredol, M.; Kynast, U.; Ronda, C. *Adv. Mater.* **1991**, *3*, 361−367.
(5) Dance, I. G.; Fisher, K. *Prog. Inorg. Chem.* **1994**, *41*, 637−803.
(6) Dance, I. G. *Polyhedron* **1986**, *5*, 1037.
(7) Steigerwald, M. L.; Brus, L. E. *Annu. Rev. Mater. Sci.* **1989**, *19*, 471.
(8) Weller, H. *Angew. Chem., Int. Ed. Engl.* **1993**, *32*, 41−53.
(9) West, A. R. *Solid State Chemistry and its Applications*; John Wiley & Sons Ltd.: New York, 1984.
(10) Nyman, M.; Hampden-Smith, M. J.; Duesler, E. N. *Inorg. Chem.* **1995**, *35*, 802−803.
(11) Dance, I. G.; Choy, A.; Scudder, M. L. *J. Am. Chem. Soc.* **1984**, *106*, 6825.
(12) Herron, N.; Calabrese, J. G.; Farneth, W. E.; Wang, Y. *Science* **1993**, *259*, 1426.
(13) Murray, C. B.; Norris, D. J.; Bawendi, M. G. *J. Am. Chem. Soc.* **1993**, *115*, 8706−8715.
(14) Steigerwald, M. L.; Brus, L. E. *Acc. Chem. Res.* **1990**, *23*, 183.

S0020-1669(96)00784-7 CCC: $14.00

°C)[15] and $Cd(SOCC(CH_3)_3)_2$TMEDA and $Zn(SOCC(CH_3)_3)_2$-TMEDA as precursors for formation of $Cd_{1-x}Zn_xS$ thin films with compositional control.[16] This report focuses on the synthesis and characterization of the lutidine adducts, $Zn(SOCCH_3)_2Lut_2$, $Cd(SOCCH_3)_2Lut_2$, $Zn(SOCC(CH_3)_3)_2Lut_2$, and $Cd(SOCC(CH_3)_3)_2Lut_2$ (Lut = 3,5-dimethylpyridine or 3,5-lutidine), and their thermal reactivity in solution and the solid state.

Experimental Section

General Procedures and Instrumentation. Standard Schlenk line and inert-atmosphere box procedures were used for handling of diethylzinc. Thioacetic acid was purchased from Aldrich and distilled twice prior to use to remove yellow-colored impurities. Thiopivalic acid was synthesized by the reaction of H_2S and trimethylacetyl chloride and distilled twice to remove orange-colored impurities.[17] All solvents used for syntheses (3,5-lutidine, toluene, pentane) were distilled from sodium−diphenyl ketone and stored over predried 4 Å molecular sieves. Metal thiocarboxylate species were typically characterized by carbon, hydrogen, and nitrogen elemental analyses, thermogravimetric analysis, ^1H, ^{13}C, and ^{113}Cd (where appropriate) nuclear magnetic resonance (NMR) spectroscopy, FTIR, and single-crystal X-ray diffraction for structural analysis. Carbon, hydrogen, and nitrogen elemental analyses were carried out on a Perkin-Elmer 2400 elemental analyzer. Thermogravimetric analyses (TGA) were performed on a Perkin-Elmer TGA 7700 thermogravimetric analyzer. The NMR data were recorded on a Bruker AC-250. Deuterated NMR solvents were predried, and peaks were referenced internally to the residual protio impurity of the deuterated solvent. The ^{113}Cd NMR spectra were recorded using an inverse-gated decoupling pulse program to accommodate the negative NOE of the ^{113}Cd nucleus ($\gamma = -0.6217$). The ^{113}Cd peaks were referenced externally to an aqueous solution of $Cd(SO_4)$ (5 ppm). Single-crystal X-ray diffraction data were collected on a Siemens R3m/V diffractometer in the Department of Chemistry at the University of New Mexico.

Synthesis of $M(SOCR)_2Lut_2$ (M = Cd, Zn; R = CH_3, $C(CH_3)_3$; Lut = 3,5-Lutidine) $Cd(SOCCH_3)_2Lut_2$. Cadmium carbonate (1.0 g, 5.8 mmol), 3,5-lutidine (1.2 g, 11.6 mmol), and 20 mL of toluene were combined in a round-bottomed flask. Thioacetic acid (0.9 g, 11.6 mmol) was dropped into the mixture while stirring rapidly, and stirring was continued for 1 h at room temperature. As the reaction proceeded, the solid cadmium carbonate disappeared, CO_2 bubble formation was observed, and the resulting clear solution became yellow. The toluene and volatile byproducts of the reaction (water) were removed under reduced pressure, and a white crystalline solid and a small amount of yellow material shown to be cadmium sulfide remained. The solid was redissolved in toluene and filtered to remove the cadmium sulfide. The solution was then placed in the freezer and yielded colorless, crystalline blocks. Yields ranged from ∼2.0−2.5 g (59−74% yield based on cadmium carbonate).

Analytical Data. Anal. Calcd: C, 45.34; H, 5.04; N, 5.88. Found: C, 45.30; H, 5.14; N, 5.68. Thermogravimetric analysis: The sample of $Cd(SOCCH_3)_2Lut_2$ decomposed in one step at ∼150 °C with 32% wt remaining ($MW(CdS)/MW(Cd(SOCCH_3)_2Lut_2) \times 100 = 30\%$. The inorganic residue in the TGA pan was identified as hexagonal CdS by powder X-ray diffraction. NMR data (C_6D_6): ^1H NMR, 1.69 ppm [12H, C*H*$_3$-lutidine], 2.58 ppm [6H, SOCC*H*$_3$], 6.55 ppm [2H, lutidine para-CH], 8.50 ppm [4H, lutidine ortho-CH]; ^{13}C NMR, 17.8 ppm [*C*H$_3$-lutidine], 35.1 ppm [SOCC*H*$_3$], 133.7 ppm [*C*-CH$_3$-lutidine], 138.8 ppm [para-*C*H-lutidine], 147.7 ppm [ortho *C*H-lutidine]; ^{113}Cd NMR, 353.5 ppm.

$Zn(SOCCH_3)_2Lut_2$. Diethylzinc (1.0 g, 8.1 mmol), lutidine (1.7 g, 16.2 mmol), and 20 mL of toluene were combined in a round-bottomed flask in an inert-atmosphere box. The flask was removed from the inert-atmosphere box and placed in an ice water bath. Thioacetic acid (1.2 mL, 16.2 mmol) was added to the solution via a pipet while stirring, and a white precipitation formed immediately. The solution was warmed to room temperature while stirring. After several hours, the solution was heated to 60 °C to dissolve most of the reaction product, and the hot solution was filtered immediately. The product crystallized at room temperature overnight as small colorless blocks. Yield: 2.7 g (78% yield based on diethyl zinc).

Analytical Data. Anal. Calcd: C, 50.30; H, 5.59; N, 6.52. Found: C, 50.40; H, 5.70; N, 6.37. Thermogravimetric analysis: The sample of $Zn(SOCCH_3)_2Lut_2$ decomposed in one step around 175 °C with 25% wt remaining ($MW(ZnS)/MW(Zn(SOCCH_3)_2Lut_2) \times 100 = 23\%$. The inorganic residue in the TGA pan was identified as poorly crystalline wurtzite or sphalerite ZnS by powder X-ray diffraction. NMR data (C_6D_6): ^1H NMR, 1.63 ppm [12H, C*H*$_3$-lutidine], 2.55 ppm [6H, SOCC*H*$_3$], 6.47 ppm [2H, lutidine para-CH], 8.78 ppm [4H, lutidine ortho-CH]; ^{13}C NMR, 17.8 ppm [*C*H$_3$-lutidine], 36.1 ppm [SOCC*H*$_3$], 134.3 ppm [*C*-CH$_3$-lutidine], 140.1 ppm [para-*C*H-lutidine], 147.4 ppm [ortho-*C*H-lutidine].

$Cd(SOCC(CH_3)_3)_2Lut_2$. Cadmium carbonate (1.0 g, 5.8 mmol), lutidine (1.2 g, 11.6 mmol), and 20 mL of toluene were combined in a round-bottomed flask. Thiopivalic acid (1.5 mL, 11.8 mmol) was pipetted into the rapidly stirring mixture. After approximately 40 min, the solution become clear and yellow, and gas evolution (CO_2) was observed over the course of the reaction. After the mixture was stirred for 160 min, the toluene and volatile byproducts (water) were removed under reduced pressure and a glassy, white solid remained. The solid was redissolved in toluene, and pentane vapor was introduced slowly. After 4 days, $Cd(SOCC(CH_3)_3)_2Lut_2$ crystallized as long, colorless blades. Yield: 2.2 g (68% yield based on cadmium carbonate).

Analytical Data. Anal. Calcd: C, 51.4; H, 6.42; N, 5.00. Found: C, 51.29; H, 6.60; N, 4.88. The sample of $Cd(SOCC(CH_3)_3)_2Lut_2$ decomposed in one step around 150 °C with 27% wt remaining ($MW(CdS)/MW(Cd(SOCC(CH_3)_3)_2Lut_2) \times 100 = 26\%$. The inorganic residue in the TGA pan was identified as well-crystallized hexagonal CdS by powder X-ray diffraction. NMR data (C_6D_6): ^1H NMR, 1.50 ppm [18H, SOCC(C*H*$_3$)$_3$], 1.65 ppm [12H, C*H*$_3$-lutidine], 6.47 ppm [2H, lutidine para-CH], 8.53 ppm [4H, lutidine ortho-CH]; ^{13}C NMR, 17.8 ppm [*C*H$_3$-lutidine], 29.6 ppm [SOCC(*C*H$_3$)$_3$], 47.9 ppm [SOCC(*C*H$_3$)$_3$], 134.0 [*C*-CH$_3$-lutidine], 138.4 ppm [para-*C*H-lutidine], 147.5 ppm [ortho *C*H-lutidine]; ^{113}Cd NMR, 338.6 ppm.

$Zn(SOCC(CH_3)_3)_2Lut_2$. Diethylzinc (1.0 g, 8.1 mmol), lutidine (1.7 g, 16.2 mmol), and 20 mL of toluene were combined in a round-bottomed flask in an inert-atmosphere box. The flask was removed from the inert-atmosphere box and placed in an ice water bath. Thiopivalic acid (2.1 mL, 16.2 mmol) was added to the stirring solution via a pipet, and a pale yellow solution formed. The solution was warmed to room temperature while stirring for several hours and placed in the freezer. Large, block-shaped colorless crystals of $Zn(SOCC(CH_3)_3)_2Lut_2$ formed overnight. Yield: 3.5 g (84% based on diethylzinc).

Analytical Data. Anal. Calcd: C, 56.10; H, 7.01; N, 5.45. Found: C, 56.09; H, 7.12; N, 5.37. The sample of $Zn(SOCC(CH_3)_3)_2Lut_2$ decomposed in one step around 200 °C with 20% wt remaining ($MW(CdS)/MW(Cd(SOCC(CH_3)_3)_2Lut_2) \times 100 = 19\%$. The inorganic residue in the TGA pan was identified as poorly crystalline wurtzite or sphalerite ZnS by powder X-ray diffraction. NMR data (C_6D_6): ^1H NMR, 1.40 ppm [18H, SOCC(C*H*$_3$)$_3$], 1.65 ppm [12H, C*H*$_3$-lutidine], 6.51 ppm [2H, lutidine para-CH], 8.69 ppm [4H, lutidine ortho-CH]; ^{13}C NMR, 17.8 ppm [*C*H$_3$-lutidine], 29.3 ppm [SOCC(*C*H$_3$)$_3$], 48.2 ppm [SOCC(*C*H$_3$)$_3$], 134.02 [*C*-CH$_3$-lutidine], 140.1 ppm [para-*C*H-lutidine], 147.3 ppm [ortho *C*H-lutidine].

Single-Crystal X-ray Diffraction Data. Crystallographic data for the four species are summarized in Table 1. Relevant bond angles and lengths for $Cd(SOCCH_3)_2Lut_2$, $Zn(SOCCH_3)_2Lut_2$, $Cd(SOCC(CH_3)_3)_2Lut_2$ and $Zn(SOCC(CH_3)_3)_2Lut_2$ are listed in Tables 2−5, respectively. SHELXL software was used for all computations (G. Sheldrick, Siemens XRD, Madison, WI).

$Cd(SOCCH_3)_2Lut_2$. In initial refinement cycles, all non-hydrogen atoms were refined isotropically and then all non-hydrogen atoms were refined anisotropically and hydrogen atoms were not included. For the final refinement, all non-hydrogen atoms were refined anisotropi-

(15) Nyman, M.; Hampden-Smith, M. J.; Duesler, E. N. *Adv. Mater. CVD* **1996**, *2*, 171−174.
(16) Nyman, M.; Hampden-Smith, M. J.; Duesler, E. N. Manuscript in preparation.
(17) Bochmann, M.; Bwembya, G. C.; Grinter, R.; Powell, A. K.; Webb, K. J. *Inorg. Chem.* **1994**, *33*, 2290−2296.

Table 1. Summary of Crystallographic Data

	$Cd(SOCCH_3)_2Lut_2$	$Zn(SOCCH_3)_2Lut_2$	$Cd(SOCC(CH_3)_2Lut_2$	$Zn(SOCC(CH_3)_2Lut_2$
formula	$C_{18}H_{24}CdN_2O_2S_2$	$C_{18}H_{24}N_2O_2S_2Zn$	$C_{24}H_{36}CdN_2S_2O_2$	$C_{24}H_{36}N_2S_2O_2Zn$
fw	476.9	429.9	561.1	514.0
color, habit	colorless, transparent prism	colorless, transparent prism	colorless, transparent prism	colorless, transparent prism
a, Å	8.267(1)	8.146(1)	18.666(1)	9.855(1)
b, Å	9.467(1)	9.472(1)	9.380(1)	10.719(1)
c, Å	14.087(1)	14.008(1)	16.542(1)	14.125(1)
α, deg	94.04(1)	94.21(1)		91.94(1)
β, deg	91.49(1)	90.99(1)	94.42(1)	104.14(1)
γ, deg	104.03(1)	104.35(1)		105.50(1)
cryst system	triclinic	triclinic	monoclinic	triclinic
space group	$P\bar{1}$	$P\bar{1}$	*C*2/*c*	$P\bar{1}$
T/K	293	293	293	293
λ/Å	0.710 73	0.710 73	0.710 73	0.710 73
Z	2	2	4	2
cryst size/mm	0.48 × 0.60 × 0.67	0.23 × 0.34 × 0.46	0.36 × 0.46 × 0.50	0.16 × 0.18 × 0.20
V, $Å^3$	1066.0(2)	1043.5(2)	2887.7(4)	1386.4(2)
indep reflcns	4903	3681	2552	4871
obsd reflcns	4415	2912	2194	2614
abs coeff, mm^{-1}	1.233	1.390	0.921	1.057
R(*F*), %[a]	3.07	3.40	4.18	4.97
$R_w(F)$, %[b]	3.00	3.21	4.23	4.02
GOF	1.28	1.34	1.18	1.07

[a] $R = \sum\Delta F/\sum F_o$. [b] $R_w = \sum w^{1/2}\Delta F/\sum w^{1/2}F_o$ ($F > 2.0\sigma(F)$).

Table 2. Relevant Bond Lengths (Å) and Angles (deg) for $Cd(SOCCH_3)_2Lut_2$

Bond Lengths			
Cd−S(1)	2.487(1)	Cd−N(1)	2.293(1)
Cd−S(2)	2.496(1)	Cd−N(2)	2.288(1)
S(1)−C(1)	1.745(3)	O(1)−C(1)	1.221(4)
O(2)−C(3)	1.217(4)	S(2)−C(3)	1.732(4)
Bond Angles			
S(1)−Cd−S(2)	112.0(1)	S(1)−Cd−N(1)	110.9(1)
S(2)−Cd−N(1)	107.7(1)	S(1)−Cd−N(2)	107.7(1)
S(2)−Cd−N(2)	113.8(1)	N(1)−Cd−N(2)	104.5(1)

Table 3. Relevant Bond Lengths (Å) and Angles (deg) for $Zn(SOCCH_3)_2Lut_2$

Bond Lengths			
Zn−S(1)	2.309(1)	Zn−N(1)	2.064(1)
Zn−S(2)	2.312(1)	Zn−N(2)	2.068(1)
S(1)−C(1)	1.749(4)	S(2)−C(3)	1.746(4)
O(1)−C(1)	1.213(5)	O(2)−C(3)	1.214(4)
Bond Angles			
S(1)−Zn−S(2)	109.2(1)	S(1)−Zn−N(1)	110.9(1)
S(2)−Zn−N(1)	109.2(1)	S(1)−Zn−N(2)	109.2(1)
S(2)−Zn−N(2)	112.2(1)	N(1)−Zn−N(2)	106.1(1)

Table 4. Relevant Bond Lengths (Å) and Angles (deg) for $Cd(SOCC(CH_3)_3)_2Lut_2$

Bond Lengths			
Cd−S	2.489(1)	Cd−N	2.340(3)
S−C(1)	1.719(5)	O−C(1)	1.215(6)
Bond Angles			
S−Cd−SA	133.4(1)	S−Cd−N	103.2(1)
S−Cd−NA	108.8(1)	N−Cd−SA	108.8(1)
SA−Cd−NA	103.2(1)	N−Cd−NA	91.5(2)

cally and all hydrogen atoms included in idealized positions (riding model) with the isotropic *U* of hydrogens set to 1.25*U* of the parent atom.

$Zn(SOCCH_3)_2Lut_2$. The refinement was performed in the same manner as that described above except that the 001 reflection fitted poorly and it was omitted from the final refinement cycle.

$Cd(SOCC(CH_3)_3)_2Lut_2$. In initial refinement cycles, all non-hydrogen atoms were refined isotropically. The following atoms show large resulting isotropic *U*'s ($Å^2$): C(3), 0.14; C(4), 0.19; C(5), 0.23; C(12), 0.13; O, 0.10. The difference map shows second positions for C(3), C(4), and C(5). The non-hydrogen atoms were refined isotropically with disorder on C(3), C(4), and C(5) by varying occupation and fixing the isotropic *U*. Then all non-hydrogen atoms were refined anisotropically and hydrogen atoms were not included and the occupancy on primary and secondary disordered positions were at 0.586 45, 0.413 55, and 0.106 28, respectively. Some atoms show very anisotropic *U*'s and the difference maps were examined for possible disorder involving these atoms, but no other positions were found. For the final refinement, all non-hydrogen atoms were refined anisotropically and all hydrogen atoms included in idealized positions (riding model) with the isotropic *U* of hydrogens set to 1.25*U* of the parent atom.

Table 5. Relevant Bond Lengths (Å) and Angles (deg) for $Zn(SOCC(CH_3)_3)_2Lut_2$

Bond Lengths			
Zn−S(1)	2.294(4)	Zn−N(1)	2.072(4)
Zn−S(2)	2.313(1)	Zn−N(2)	2.084(5)
Zn−S(1′)	2.273(5)	S(1)−C(15)	1.743(6)
S(1/)−C(15)	1.746(7)	S(2)−C(20)	1.738(7)
Bond Angles			
S(1)−Zn−S(2)	117.6(1)	S(1)−Zn−N(1)	109.5(2)
S(1)−Zn−N(2)	117.2(2)	S(2)−Zn−N(1)	110.7(1)
S(2)−Zn−N(2)	101.6(1)	N(1)−Zn−N(2)	98.6(2)
S(1)−Zn−S(1/)	13.6(1)	S(1/)−Zn−S(2)	113.8(1)
S(1/)−Zn−N(1)	121.7(2)	S(1/)−Zn−N(2)	107.2(2)

$Zn(SOCC(CH_3)_3)_2Lut_2$. In initial refinement cycles, all non-hydrogen atoms were refined isotropically. The following atoms show large resulting isotropic *U*'s ($Å^2$): S(1), 0.09; C(17), 0.20; C(18), 0.18; C(19), 0.16; C(22), 0.17; C(23), 0.16; C(24), 0.15. The non-hydrogen atoms were refined isotropically with disorder on S(1), C(17), C(18), C(19), C(22), C(23), and C(24) by varying occupation and fixing the isotropic *U*. Then all non-hydrogen atoms were refined anisotropically with fixed occupancy for disordered atoms with varying *U*'s. For the final refinement, all non-hydrogen atoms were refined anisotropically and all hydrogen atoms included in idealized positions (riding model) with the isotropic *U* of hydrogens set to 1.25*U* of the parent atom. The disordered atoms had fixed calculated positions, and the reflection (001) was omitted from the refinement (considered a bad reflection).

Thermal Decomposition Studies of $M(SOCR)_2Lut_2$. Thermal decomposition of each compound was studied in the solid state through thermogravimetric analysis experiments and in solution by ^1H NMR spectroscopy using pyridine-d_5 and toluene-d_8 as solvents. Typical TGA experiments were carried out by heating the sample from 30 to 600 °C at a rate of 10 °C/min under a dinitrogen purge. Any crystalline phases in the material remaining in the TGA sample pan after heating to 600 °C were identified by powder X-ray diffraction. Solutions for thermal decomposition studies were prepared by dissolving approximately 10 mg of sample in 0.7 mL of deuterated solvent in an inert-atmosphere box, and the tubes were capped with rubber septa. The capped NMR tube samples were removed from the inert-atmosphere box and heated overnight in an oil bath at 110 °C. For several select samples, the experiments were carried out with rigorous exclusion of water to ensure reaction products are not affected by trace amounts of water. Sample preparations included pretreating the NMR tubes with hexamethyldisilazane to remove surface hydroxyl groups from the glass tube and sealing the tubes under vacuum. Reactants and products in solution were examined by ^{1}H NMR before and after heating, respectively. Products of thermal decomposition which precipitated were examined by powder X-ray diffraction and/or TEM. The powder X-ray diffraction data were obtained on a Siemens D5000 operated at 35 kV with a Cu Kα source (1.5406 Å). Typical scan parameters included 10−90° (2θ) scan, 0.02° step size, and 6 s step time. Powder samples were smear-mounted on a glass slide. High-resolution transmission electron microscopy (HRTEM) was carried out on a JEOL-2010 instrument operated at 200 kV. Samples were mounted on a holey carbon grid, either as a dry powder or a drop of solution from which the solvent evaporated.

Results and Discussion

Synthesis and Characterization of M(SOCR)$_2$Lut$_2$. The reactions of $ZnEt_2$ with the thioacetic and thiopivalic acids resulted in nearly quantitative yields of pure, highly crystalline product, since the only byproduct is ethane which can be removed easily. The cadmium compounds were isolated in lower yields since they tend to decompose to CdS slowly in solution under these conditions. Additionally, water is a byproduct of the reaction of cadmium carbonate with the thiocarboxylic acid, which might accelerate the decomposition. Cadmium-113 NMR chemical shifts were in the region of 350 ppm for these compounds and the analogous TMEDA compounds,[15] which is typical for cadmium in a tetrahedral CdS_4N_4 environment.[18−20] No Cd−H coupling was observed for these compounds since the nearest hydrogen was 4 bonds away from the cadmium. The infrared spectra for crystalline samples showed the presence of bands mainly above 1620 cm^{-1} which were assigned to uncoordinated ν(C═O) in thiocarboxylate carbonyls, and the ν(C−S) bands were found around 960 cm^{-1} consistent with coordinated ν(C−S). All C, N, and H elemental analyses agreed with the calculated values for the proposed empirical formulas within experimental error.

Solid-State Structures of M(SOCR)$_2$Lut$_2$. All M(SOCR)$_2$L$_2$ (M = Zn, Cd; R = CH_3, $C(CH_3)_3$; L = 3,5-lutidine or L$_2$ = TMEDA) species which we have synthesized and characterized thus far have the same metal coordination number and bonding modes of the thiocarboxylate ligands. The complexes are monomeric, with approximately tetrahedral metal centers, and the thiocarboxylate ligands are monodentate with sulfur bonded to the metal. Several factors influence the thiocarboxylate bonding mode including the hard/soft nature of the metal, the preferred coordination number of the metal, and the preferred conformation of the ligand (i.e. stability of the C−O double bond vs stability of the C−S double bond). When one considers these factors, the bonding modes exhibited by this set of molecular compounds is somewhat surprising. For example, cadmium commonly exhibits coordination numbers greater than 4 and Zn(II) is “harder” and less thiophillic than the Cd(II). Consideration of these factors led us to expect a greater variety in the bonding mode of the thiocarboxylate ligands in these complexes, but this was not observed. However, the bonding mode which the thiocarboxylate ligands adopt appears to be ideal for thiocarboxylic anhydride elimination reactions to form metal sulfide materials.

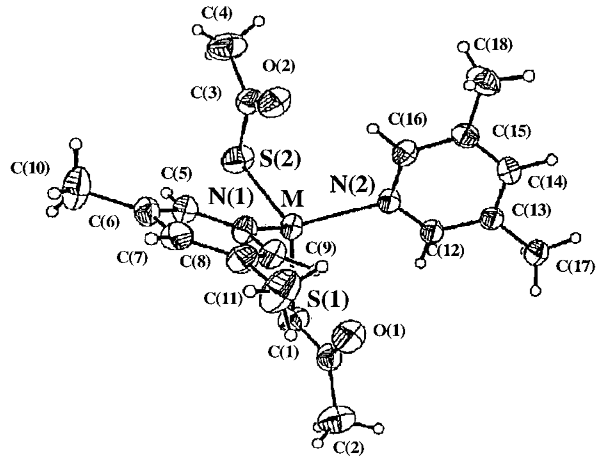

Figure 1. Molecular structure of M(SOCCH$_3$)$_2$Lut$_2$ (M = Zn, Cd).

The structure of the M(SOCCH$_3$)$_2$Lut$_2$ (M = Zn, Cd) molecules determined by single-crystal X-ray diffraction is shown in Figure 1. The zinc and the cadmium analogs are isostructural. Both molecules crystallize in a triclinic crystal system with $P\bar{1}$ symmetry and 2 molecules in the unit cell. The unit cell parameters of the two compounds are very similar, with slightly larger values for the cadmium compound. Both the zinc and the cadmium molecules are approximately tetrahedral with approximate C_{2v} molecular symmetry where the molecular 2-fold axis bisects the S−M−S and the N−M−N angles.

The molecular structures of Zn(SOC(CH$_3$)$_3$)$_2$Lut$_2$ and Cd(SOC(CH$_3$)$_3$)$_2$Lut$_2$ are similar to the thioacetate compounds; the zinc species crystallizes in a triclinic crystal system with $P\bar{1}$ symmetry and 2 molecules in the unit cell. The coordination environment about the metal center is a distorted tetrahedron with a molecular 2-fold axis bisecting the N−Zn−N angle and the S−Zn−S angle. The cadmium crystallizes in a monoclinic crystal system with $C2/c$ symmetry and 4 molecules per unit cell. The *tert*-butyl groups are disordered over 2 sites. The distorted tetrahedral molecule has a 2-fold axis bisecting the N−Cd−N angle (91.5(2)°) and the S−Cd−S angle (133.4(1)°).

The structural characteristics of the compounds reported here are consistent with the structural data for other examples of metal thiocarboxylate derivatives available in the literature. The propensity for monodentate S-bonded thiocarboxylate ligands is observed in all but one of the compounds that we have recently reported as precursors to metal sulfide materials, including derivatives of Ca, Sr, Ba,[21] Ga,[22] In,[23] Sn, Pb,[24] Zn, and Cd.[15] Other structurally characterized zinc(II) thiocarboxylate compounds, namely Zn(pz*)(SOCMe), where pz* = tris(3-phenylpyrazolyl)borate),[25] and Zn(SOCPh)$_2$(H$_2$O)$_2$[26] as well as Co ([Co(SOCMe)$_2$(tren)]$^+$)[27] and Sb (SbPh(SOMe)$_2$)[28]

(18) Ramli, E.; Rauchfuss, T. B. *J. Am. Chem. Soc.* **1990**, *112*, 4043.
(19) Sola, J.; Gonzalez-Duarte, P.; Sanz, J.; Casals, I.; Alsina, T.; Sobrados, I.; Alvarez-Larena, A.; Piniella, J. F.; Sonans, X. *J. Am. Chem. Soc.* **1993**, *115*, 10018−10028.
(20) Reger, D.; Myers, S.; Mason, S.; Rheingold, A.; Haggerty, B. *Inorg. Chem.* **1995**, *34*, 4996−5002.
(21) So, J. H.; Boudjouk, P. *Inorg. Chem.* **1990**, *29*, 1592−1593.
(22) Zhou, H. S.; Sasahara, H.; Honma, I.; Komiyama, H. *Chem. Mater.* **1994**, *6*, 1534−1541.
(23) Meyer, M.; Wallberg, C.; Kurihara, K.; Fendler, J. H. *J. Chem. Soc., Chem. Commun.* **1984**, 90−91.
(24) Ouhadi, T.; Hubert, A. J.; Teyssie, P.; Derouane, E. G. *J. Am. Chem. Soc.* **1973**, *34*, 449−453.
(25) Ouhadi, T.; Bioul, J. P.; Stevens, C.; Warin, R.; Hocks, L.; Teyssie, P. *Inorg. Chim. Acta* **1976**, *19*, 203.
(26) Sherif, F. G.; Herman, H. *Mater. Res. Soc. Symp. Proc.* **1990**, *180*, 831.
(27) Chandler, C. D.; Roger, C.; Hampden-Smith, M. J. *Chem. Rev.* **1993**, *93*, 1205.
(28) Ma, L.; Payne, D. A. *Chem. Mater.* **1994**, *6*, 875.

Table 6. Thermal Decomposition Products of $M(SOCR)_2L_2$ in Solution

$M(SOCR)_2L_2$	solvent (deuterated)	% decompn	decomp products in soln	precipitated decompn products
$Cd(SOCCH_3)_2Lut_2$	toluene	100% decomp	thioacetic anhydride, acetone	sphalerite CdS 50 Å crystallite size
$Zn(SOCCH_3)_2Lut_2$	toluene	∼60% decomp	thioacetic anhydride, acetone	amorphous "ZnS" ∼50 Å after annealing at 500 °C
$Cd(SOC(CH_3)_3)_2Lut_2$	toluene	∼25% decomp	*tert*-butylthioacetic anhydride, tetramethylpentan-3-one	sphalerite CdS 50 Å crystallite size
$Zn(SOC(CH_3)_3)_2Lut_2$	toluene	no decomp		
$Cd(SOCCH_3)_2Lut_2$	pyridine	∼80% decomp	*tert*-butylthioacetic anhydride, tetramethylpentan-3-one	100 Å sphalerite CdS
$Zn(SOCCH_3)_2Lut_2$	pyridine	no decomp		
$Cd(SOC(CH_3)_3)_2Lut_2$	pyridine	no decomp		
$Zn(SOC(CH_3)_3)_2Lut_2$	pyridine	no decomp		

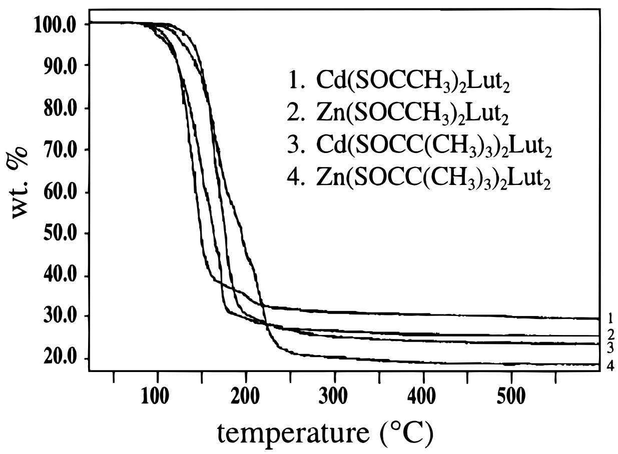

Figure 2. Thermogravimetric analysis of $Cd(SOCCH_3)_2Lut_2$, $Zn(SOCCH_3)_2Lut_2$, $Cd(SOCC(CH_3)_3)_2Lut_2$, and $Zn(SOCC(CH_3)_3)_2Lut_2$.

derivatives, also contain only monodentate S-bonded SOCR ligands. In the case of the Zn(II) and Cd(II) compounds reported here, the M−S distances are shorter than the sum of the M−S covalent radii and the C═O distances are in the range expected for the presence of a double bond.

Solid-State Thermal Decomposition Studies of $M(SOCR)_2L_2$. The thermogravimetric analyses for $Zn(SOCCH_3)_2Lut_2$, $Cd(SOCCH_3)_2Lut_2$, $Zn(SOC(CH_3)_3)_2Lut_2$, and $Cd(SOC(CH_3)_3)_2Lut_2$ are shown in Figure 2. All compounds decompose between 150 and 200 °C, and the final weight remaining for each sample agrees within 5 wt % with the amount required for the formation of metal sulfide (details for each are listed in the Experimental Section) consistent with eqs 1 and 2. Powder X-ray diffraction of the inorganic residues confirmed this result, in that only crystalline MS was observed, with no evidence for the corresponding metal oxide. In general, the zinc species formed poorly crystalline, wurtzite and/or sphalerite ZnS as evidenced by the broad X-ray diffraction peaks. The CdS formed on thermal decomposition of the cadmium compounds was better crystallized than the thermal decomposition products of the zinc analogs. The CdS was the wurtzite phase, distinguished from the sphalerite phase by the (100) and (101) peaks, which are unique to the diffraction pattern of the wurtzite phase and not present in the diffraction pattern of the sphalerite phase. This is not surprising since hexagonal CdS is the thermodynamically stable phase under these preparation conditions.

The absence of crystalline ZnO and CdO in the solid-state thermal decomposition products of the $Zn(SOCR)_2L_2$ and $Cd(SOCR)_2L_2$, respectively, suggests that these are logical precursors to MS materials. Since no metal oxides are formed in solid-state or in solution decomposition (see below), this suggests that the oxygen present in these ligands is not disadvantageous, likely because the carbon−sulfur bond is more labile than the carbon−oxygen double bond and the molecule is more likely to undergo $(COR)_2S$ elimination rather than the some alternative which would lead to the formation of metal oxide (i.e. $(CSR)_2O$ elimination). The temperature of thermal decomposition which was observed by TGA is sufficiently low so that thermolysis of the neutral ligands (lutidine), which could result in impurity incorporation, is not likely to occur.

Thermal Decomposition Studies of $M(SOCR)_2L_2$ in Solution. The thermal decomposition products obtained on heating solutions of these compounds at 110 °C for 12 h are summarized in Table 6. These experiments were conducted generally in deuterated solvents in NMR tubes. Experiments were carried out using NMR tubes that had been washed and dried in the normal way and also those treated with silylating agents (Me_3SiNMe_2) to remove surface hydroxyl groups from the glass walls. In both cases, identical results were obtained. The degree of decomposition for the various $M(SOCR)_2Lut_2$ species is observed by the ratio of the precursor remaining after heating. Under a given set of conditions, we observe the following: (1) Cd compounds decompose more readily than Zn compounds. (2) Thioacetate ($R = CH_3$) compounds decompose more readily than thiopivalate compounds ($R = C(CH_3)_3$). (3) Decomposition takes place more readily in toluene than pyridine.

The major decomposition product of the thioacetate compounds ($R = CH_3$) is thioacetic anhydride ($S(COCH_3)_2$). Acetone is also observed after heating for extended periods. The thioacetic anhydride was identified by the ^{1}H NMR CH_3 peak at 1.95 ppm in toluene-d_8 and 2.44 ppm in pyridine-d_5. This result was confirmed by adding a sample of authentic thioacetic anhydride (Aldrich no. A2,220-3) to the solution. The other decomposition product present in both the pyridine ($CO(CH_3)_2$, 2.13 ppm) and toluene ($CO(CH_3)_2$ 1.98 ppm) solution after extended heating is acetone. Acetone was identified by adding an authentic sample of acetone to a solution containing the decomposition products. The sum of the integrated areas of the thioacetic anhydride methyl peak, the acetone methyl peak, and the remaining thioacetate methyl peak (in the case of partially decomposed samples) is equal to the integrated intensity of the original thioacetate methyl peak and is also consistent when compared to the area of the CH_3-lutidine peak. These observations support the conclusion that thioacetic anhydride and acetone are the sole decomposition products of $M(SOCR)_2$. Evidence that thioacetic anhydride is formed first and that acetone is formed from thermal decomposition of thioacetic anhydride was obtained by monitoring the contents of these solution as a function of time. For example, Figure 3, shows thermal decomposition of $Cd(SOCCH_3)_2Lut_2$ in an in-situ heating (55 °C) ^{1}H NMR experiment in a toluene-d_8 solution. The thioacetic anhydride peak (1.95 ppm) grows proportionally with disappearance of the Cd−$SOCCH_3$ peak (2.58 ppm). Additionally, when an authentic sample of thioacetic anhydride is heated, the conversion to acetone over time occurs at the expense of the thioacetic anhydride peaks. Decomposition of thioacetic anhydride to acetone is observed to take place more rapidly in pyridine than in toluene, both in the presence and the absence of $M(SOCR)_2L_2$. The formation of acetone requires

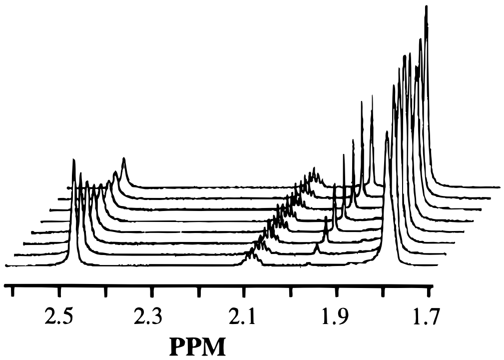

Figure 3. Thermal decomposition of $Cd(SOCCH_3)_2Lut_2$ in an in-situ heating (55 °C) ^{1}H NMR experiment in a toluene-d_8 solution. The $S(COCH_3)_2$ peak (1.95 ppm) grows proportionally with the disappearance of the Cd−$SOCCH_3$ peak (2.58 ppm). Other peaks are *methyl*-lutidine at 1.81 ppm and residual protio *methyl*-toluene at 2.09 ppm (quintet).

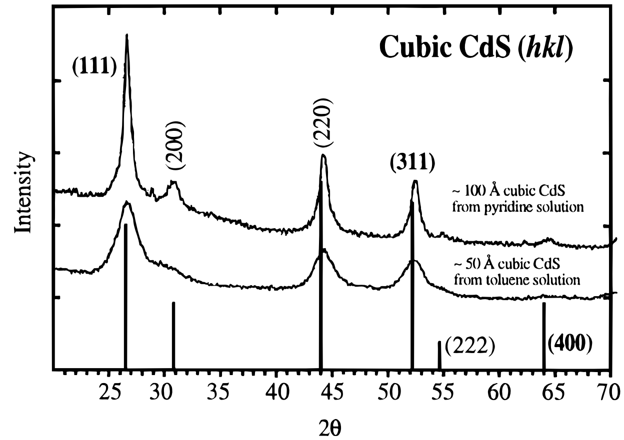

Figure 4. X-ray diffraction spectra of the sphalerite CdS powders precipitated from toluene (bottom) and pyridine (top) solutions of Cd-$(SOCCH_3)_2Lut_2$.

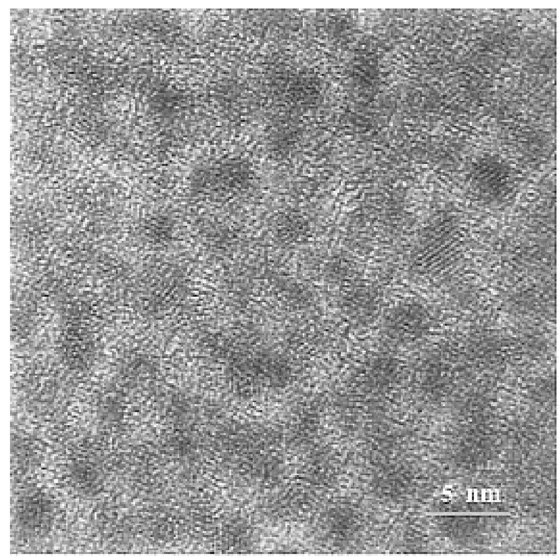

Figure 5. TEM image of sphalerite CdS nanocrystals formed from $Cd(SOCCH_3)_2Lut_2$ in toluene. Sphalerite CdS 111 $d \sim 3.35$ Å.

the presence of other decomposition products such as COS and/or CO with elemental sulfur as previously reported in the literature.[29]

The analogous products, thiopivalic anhydride ($S(COC(CH_3)_3)_2$), 1.0 ppm) and 2,2,4,4-tetramethylpentan-3-one ($CO(C(CH_3)_3)_2$), 1.1 ppm), are formed from thermal decomposition of the thiopivalate compounds ($R = C(CH_3)_3$) in toluene. Negligible thermal decomposition was observed for either $Zn(SOC(CH_3)_3)_2Lut_2$ or $Cd(SOC(CH_3)_3)_2Lut_2$ in pyridine. In order to confirm the identification of thiopivalic anhydride, it was synthesized[29] independently by dehydration of thiopivalic acid with P_2O_5 in hot toluene. The 2,2,4,4-tetramethylpentan-3-one was identified by spiking samples with authentic reagent (Aldrich no. 28,261-8).

The elimination of the thiocarboxylic anhydrides could occur via a number of different mechanisms, including inter- or intramolecular elimination. Preliminary studies to determine the order of the reaction suggest that the kinetic equations are complex. We observe that the rate of thioacetic anhydride elimination decreases as the concentration of the starting material increases and that the reaction rate decreases in coordinating vs noncoordinating solvent. As a result, we currently believe that the reaction mechanism requires pre-equilibrium dissociation of lutidine followed, probably, by intermolecular, rate-determining thioacetic anhydride elimination.

The product of thermally-induced thiocarboxylic anhydride elimination from $Cd(SOCR)_2Lut_2$ ($R = CH_3$, $C(CH_3)_3$) in both pyridine and toluene is nanocrystalline CdS. The X-ray diffraction spectra of the CdS powders precipitated from toluene and pyridine solutions of $Cd(SOCCH_3)_2Lut_2$ are shown in Figure 4. The sphalerite CdS phase is distinguished from the wurtzite CdS phase by the absence of the (100), (101), and (103) wurtzite peaks, which do not overlap with any peaks of the sphalerite phase, and the presence of the (200) sphalerite peak, which does not overlap with any of the wurtzite peaks. Sphalerite CdS is known to be the metastable phase, and wurtzite CdS is the stable phase;[30] both sphalerite[8] and wurtzite[13] nanocrystalline CdS have been synthesized in solution, and the reasons for formation of one phase over the other are not well understood. The sphalerite CdS nanocrystals formed in toluene and pyridine have a diameter of ~50 and ~100 Å, respectively, as calculated from the Scherrer equation. Nanocrystals formed from $Cd(SOCCH_3)_2Lut_2$ in toluene are shown in the TEM micrograph in Figure 5. The predominant d-spacing observed is 3.35 Å for (111) sphalerite CdS. The larger crystallite size formed in the pyridine solution likely results from the ability of pyridine to solvate larger crystallites during growth before aggregation and precipitation occurs. The crystallites form spherical aggregates of ~50−100 nm diameter, from both toluene and pyridine solutions.

The zinc thiocarboxylate compounds were generally less reactive than the cadmium compounds under identical reaction conditions, as can be seen in Table 6. The $Zn(SOC(CH_3)_3)_2Lut_2$ compound exhibited very little decomposition in both toluene and pyridine. Extensive heating and stirring in toluene for 36 h at 120 °C did not result in complete decomposition. However, the $Zn(SOCCH_3)_2Lut_2$ compound was reactive enough in toluene to isolate and characterize the metal-containing decomposition products. The pale yellow powder collected from thermal decomposition of $Zn(SOCCH_3)_2Lut_2$ is amorphous by X-ray diffraction. Thermogravimetric analysis of this sample heated to 500 °C at 10 °C/min shows approximately 10% wt loss. This weight loss is thought to be derived from loss of lutidine which was capping the "nanocluster" surfaces. ^{1}H NMR of the amorphous powder in pyridine reveals only the presence of 3,5-lutidine. The material remaining after TGA is sphalerite ZnS with an average crystallite size of 50 Å, as determined by X-ray diffraction.

(29) Mikolajczyk, M.; Kielbasinski, P. *J. Chem. Soc., Perkin Trans.* **1976**, *5*, 564−569.
(30) *Binary Phase Diagrams*; Massalski, T. B., Ed.; AMS International: Materials Park, OH, 1990; Vol. 2, p 1020.

Summary and Conclusions

The monomeric group 12 metal thiocarboxylate compounds, $Cd(SOCCH_3)_2Lut_2$, $Zn(SOCCH_3)_2Lut_2$, $Cd(SOCC(CH_3)_3)_2Lut_2$, and $Zn(SOCC(CH_3)_3)_2Lut_2$ (Lut = 3,5-lutidine) have been synthesized and fully characterized by ^{1}H, ^{13}C, and ^{113}Cd (when applicable) NMR, C, H, and N elemental analysis, thermogravimetric analysis, and single-crystal X-ray diffraction. Single-crystal X-ray diffraction reveals that all compounds are monomeric, with monodentate and S-bonded thiocarboxylate ligands. Each metal is bonded to two lutidine molecules and sits in a distorted tetrahedral coordination environment of MS_2N_2. These lutidine adducts of the thiocarboxylate compounds are structural analogs to the TMEDA adducts used as CVD precursors for ZnS, CdS, and $Zn_{1-x}Cd_xS$ thin films.[15,16] The monodentate lutidine ligands are more labile than the bidentate TMEDA ligands, which renders lutidine adducts more suitable for reactivity studies in solution and to molecular clusters or nanocrystalline solids, whereas TMEDA adducts are better suited for precursors to CVD-derived metal sulfide films. The structural and reactivity similarities of the lutidine adducts and TMEDA adducts provided an excellent opportunity to carry out solution phase decomposition studies in order to better understand the reactions of the CVD precursors and to extend the utility of these single-source precursors to the formation of molecular clusters and nanoclusters.

The cadmium compounds decompose in solution to form sphalerite, nanocrystalline CdS. This reaction has been observed to take place from 25 to 110 °C with increasing rate of CdS formation at elevated temperatures. It is proposed that the lutidine ligands act as a surface-capping reagent which retards growth of the clusters. The $Zn(SOCCH_3)_2Lut_2$ decomposes in toluene to form an amorphous material. Heating this material to 500 °C with loss of "surface-capping" lutidine results in formation of sphalerite ZnS with an average crystallite size of 50 Å. In a sense, the $M(SOCR)_2Lut_2$ species is truly a "single-source" precursor for nanocrystals of MS, in that the source of M, the source of S, and the surface-capping reagent are all provided in a single molecule.

Finally, these compounds studied in this work, $M(SOCR)_2L_2$ (M = Cd, Zn; R = CH_3, $C(CH_3)_3$; L_2 = 2 lutidine, TMEDA), provide some distinct advantages over alternative single-source precursors for ZnS and CdS such as the thiocarbamates,[31−39] thiophosphonates,[40] and thiolates.[17,41−43] These advantages include the following: (1) Thin films can be deposited from them by CVD at temperatures much lower than the alternative single-source precursors (150 °C vs 300−500 °C). (2) The decomposition reaction takes place in solution at <100 °C; therefore the reaction can be studied more accurately and there is a potential to isolate molecular clusters as intermediates. (3) Since the reaction takes place at low temperatures, it is not complicated by additional reactions such as ligand thermolysis which can lead to impurity incorporation into materials synthesized by solution routes or chemical vapor deposition.

Acknowledgment. We thank the Office of Naval Research for supporting this work and the Camille and Henry Dreyfus Foundation and the Air Force Office of Scientific Research for the purchase of an X-ray diffractometer.

Supporting Information Available: X-ray crystallographic files in CIF format for compounds $Cd(SOCCH_3)_2Lut_2$, $Zn(SOCCH_3)_2Lut_2$, $Cd(SOCC(CH_3)_3)_2Lut_2$, and $Zn(SOCC(CH_3)_3)_2Lut_2$ are available on the Internet only. Access information is given on any current masthead page.

IC960784A

(31) Frigo, D. M.; Khan, O. F. Z.; O'Brien, P. *J. Cryst. Growth* **1989**, *96*, 989.
(32) Malik, M. A.; O'Brien, P. *Chem. Mater.* **1991**, *3*, 999.
(33) Khan, O. F. Z.; O'Brien, P. *Polyhedron* **1991**, *10*, 325.
(34) Hursthouse, M. B.; Motevalli, M.; O'Brien, P.; Walsh, J. R.; Jones, A. C. *J. Mater. Chem.* **1991**, *1*, 139.
(35) Hursthouse, M. B.; Malik, M. A.; Motevalli, M.; O'Brien, P. *Polyhedron* **1992**, *11*, 45.
(36) O'Brien, P. In *Inorganic Materials*; Bruce, D. W., O'Hare, D., Eds.; John Wiley & Sons Ltd.: New York, 1992; p 491.
(37) Zeng, D.; Jain, A.; Hampden-Smith, M. J.; Kodas, T. T. To be submitted for publication.
(38) Zeng, D.; Hampden-Smith, M. J.; Alam, T.; Rheingold, A. L. *Polyhedron* **1994**, *13*, 2715−2730.
(39) Pike, R. D.; Cui, H.; Kershaw, R.; Dwight, K.; Wold, A.; Blanton, T. N.; Wernberg, A. A.; Gysling, H. J. *Thin Solid Films* **1993**, *224*, 221−226.
(40) Takahashi, Y.; Yuki, R.; Sugiura, M.; Motojima, S.; Sugiyama, K. *J. Cryst. Growth* **1980**, *50*, 491.
(41) Bochmann, M.; Webb, K.; Harman, M.; Hursthouse, M. B. *Angew. Chem., Int. Ed. Engl.* **1990**, *29*, 638.
(42) Bochmann, M.; Webb, K. J.; Hursthouse, M. B.; Mazid, M. *J. Chem. Soc., Dalton Trans.* **1991**, 2317.
(43) Bochmann, M.; Webb, K. J.; Hails, J. E.; Wolverson, D. *Eur. J. Solid State Inorg. Chem.* **1992**, *29*, 155−166.